JOURNAL OF SEMICONDUCTOR TECHNOLOGY AND SCIENCE, VOL. 21, NO. 4, AUGUST, 2021
https://doi.org/10.5573/JSTS.2021.21.4.279
ISSN(Print) 1598-1657
ISSN(Online) 2233-4866

A 24 GHz CMOS Receiver Front-end for In-Cabin Radar Systems

Yangji Jeon[1], Suyeon Lee[1], Jinman Myung[1], Geonwoo Park[1], Seungjik Lee[1], Ockgoo Lee[1], Hyunwon Moon[2], and Ilku Nam[1]

***Abstract*—A 24-GHz direct-conversion receiver front-end is presented for in-cabin applications. The proposed RF receiver is composed of a low-noise amplifier, an *I*/*Q* down-conversion mixer, and an *I*/*Q* local oscillator (LO) generator circuit. An inverter - type transconductor with third-order nonlinearity cancellation is applied to the *I*/*Q* down-conversion mixer to improve the linearity of the *I*/*Q* down-conversion mixer. By adopting a linear *I*/*Q* down-conversion mixer and a balanced *I*/*Q* LO generator, the 24 GHz receiver front-end obtains high linearity and good *I*/*Q* balancing performance. The receiver front-end draws 21-mA current from a 1.2-V supply voltage. It shows a conversion gain of 30.4 dB, noise figure (NF) of 4.5 dB, and an input 1-dB compression point (input P1dB) of -23 dBm in the 24-24.5 GHz range.**

***Index Terms*—CMOS, in-cabin, mm-wave, radar, receiver front-end**

I. INTRODUCTION

Recently traffic accidents due to driver's physical abnormalities are increasing. In particular, as the number of elderly drivers is increasing as we enter the aging society, research on a biometric monitoring radar system that monitors the driver's abnormal vital signs more accurately while driving to prevent traffic accidents due to the driver's condition abnormality is currently being conducted [1-5]. In order to measure the driver's heartbeat or respiration in a non-contact manner, research on a radar sensing transceiver using a millimeter wave (mm-wave) band is in progress. If the millimeter wave band is used, the size of the radar module can be reduced and high resolution characteristics can be obtained.

In order to integrate in a vehicle at low cost, it is necessary to use a direct conversion receiver that can minimize the use of external elements. Since the direct conversion receiver structure is used in the mm-wave band, the balancing characteristic between the *I*/*Q* signal paths of the mm-wave receiver is important. Since radar interference signals may exist in the 24 GHz band, a receiver front end with good linearity is required.

Therefore, a 24-GHz receiver front-end is proposed for in-cabin radar systems that can monitor driver’s vital signs such as heart rate and respiration in this paper. It was implemented using a 1-poly 8-metal RF 65-nm CMOS process. In the following sections, the circuit design and measured results of the receiver front-end are described in details.

II. PROPOSED CIRCUIT DESIGN

Fig. 1 shows the simplified block diagram of the presented 24 GHz direct-conversion receiver front-end. A direct-conversion receiver architecture is suitable for a wireless short-range monitoring systems in a car because it has high integration and low power consumption. The presented 24 GHz receiver front-end consists of a low-

Manuscript received May 6, 2021; reviewed Jul. 1, 2021; accepted Jul. 5, 2021
[1]Dept. of Electrical Engineering, Pusan National University, Busan 46241, Korea.
[2]Dept. of Electronic Engineering, Daegu University, Gyeongsan 38453, Korea
E-mail : nik@pusan.ac.kr

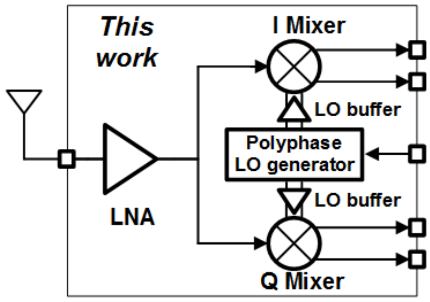

Fig. 1. Block diagram of the proposed receiver front-end.

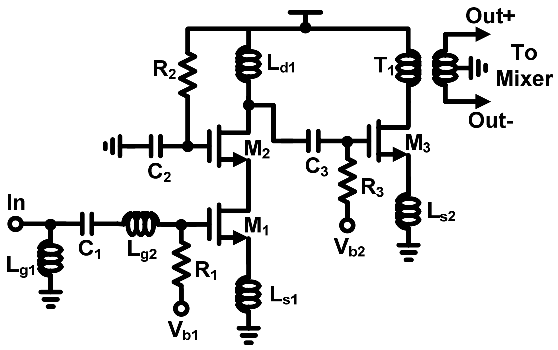

Fig. 2. Simplified schematic of the low-noise amplifier.

noise amplifier, an *I*(in-phase)/*Q*(quadrature) down-conversion mixer, and an *I*/*Q* LO generator. The RF input signal from the antenna is applied to the input of the low-noise amplifier and amplified by the low-noise amplifier. The amplified RF signal from the low-noise amplifier is converted into the baseband analog *I*/*Q* output signal using the LO input signal, which comes from an external LO signal source or an internal frequency synthesizer, by the *I*/*Q* down-conversion mixer.

The simplified schematic of a low-noise amplifier (LNA) is shown in Fig. 2. It is composed of a single-ended cascode amplifier and a single-to-differential common-source amplifier. To improve the electro-static discharge (ESD) protection performance of the LNA, the single-ended cascade amplifier with shunt inductance L_{g1} at input stage is employed. The input impedance Z_{in} of the LNA is approximately expressed as

$$\begin{aligned} Z_{in}(\omega) &= j\omega L_{g1} \,||\left[\frac{g_m L_{s1}}{C_{gs}} + j\omega\left(L_{g2}+L_{s1}\right) + \frac{1}{j\omega C_1} + \frac{1}{j\omega C_{gs}}\right] \\ &\approx j\omega L_{g1} \,||\left[\frac{g_m L_{s1}}{C_{gs}} + j\omega\left(L_{g2}+L_{s1}\right) + \frac{1}{j\omega C_{gs}}\right] \end{aligned} \tag{1}$$

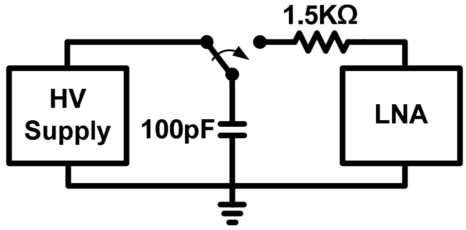

Fig. 3. Test bench for the HBM ESD simulation [7].

where g_m and C_{gs} are the transconductance and gate-source capacitance of the transistor M_1, respectively [6]. Since the value of the capacitance C_1 is much larger than that of the capacitance C_{gs}, $1/j\omega C_1$ can be ignored in Eq. (1). To make the imaginary part of (1) zero, the following Eq. (2) must be satisfied at the operating frequency f_{op};

$$f_{op} = \frac{1}{2\pi\sqrt{g_m^2 L_{s1}^2 + C_{gs}(L_{g1} + 2L_{g2} + 2L_{s1})}}. \tag{2}$$

When Eq. (2) is satisfied, Eq. (1) is can be expressed as

$$Z_{in}(\omega) \approx \frac{g_m C_{gs} L_{s1}^3}{(2g_m^2 L_{s1}^2 - C_{gs} L_{g1})[g_m^2 L_{s1}^2 + C_{gs}(L_{g1} + 2L_{g2} + 2L_{s1})]}. \tag{3}$$

Therefore, in order to match the input impedance Z_{in} of the LNA to 50 Ω, the LNA was designed by adjusting the design parameters so that Eq. (3) becomes 50 Ω.

As shown in Fig. 3, a test bench was set up for the human body model (HBM) ESD simulation [7]. In order to examine the effect of the metal width of the inductance L_{g1} on the NF and HBM characteristics of the LNA, simulation was performed by changing the metal width of the inductance L_{g1} under the same inductance condition. Fig. 4 shows the simulated NF and HBM results of the LNA according to the metal width of the inductance L_{g1}. When the metal width of L_{g1} is 2 μm, the simulated quality factor of L_{g1} is 18. When the width is 5 μm and 10 μm, the simulated quality factor of the inductor is 19 and 20, respectively. Regardless of the metal width of L_{g1}, the simulated NF of the LNA is approximately 3.2 dB, and the HBM voltage is about 200 V. Considering the NF and HBM performances of the LNA, the metal width of the inductance L_{g1} was used

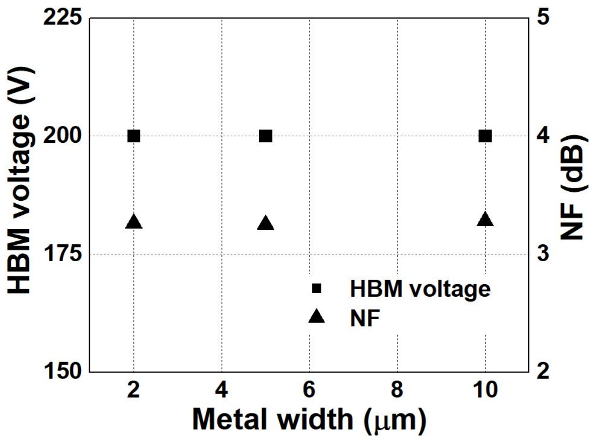

Fig. 4. Simulated human body model(HBM) test result and NF of the LNA according to the metal width of inductor L_{g1}.

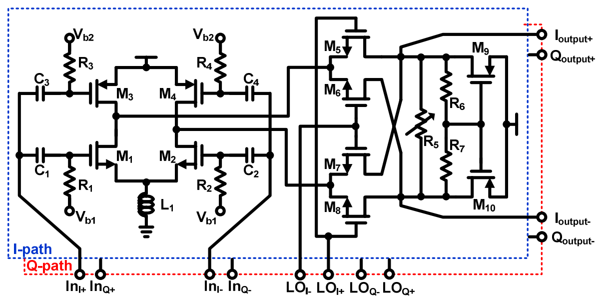

Fig. 5. Simplified schematic of the proposed I/Q down-conversion mixer.

as 2 μm in our design.

Fig. 5 shows the simplified of the proposed I/Q down-conversion mixer. An inverter-type transconductor composed of NMOS and PMOS is used at the transconductance stage of the I/Q down-conversion mixer. The inverter-type transconductor has larger transconductance than a conventional NMOS counterpart at the same dc current consumption [8, 9].

As shown in Fig. 6(a), if a small signal input voltage v_i is applied to the inverter transconductor of the down-conversion mixer, the small signal output current i_o can be expressed as

$$\begin{aligned} i_o &= i_{n1} - i_{p1} = g_m v_i + g'_m v_i^2 + g''_m v_i^3 + \cdots \\ &= \left(g_{m,n1} + g_{m,p1}\right) v_i + \left(g'_{m,n1} - g'_{m,p1}\right) v_i^2 , \\ &+ \left(g''_{m,n1} + g''_{m,p1}\right) v_i^3 + \cdots \end{aligned} \tag{4}$$

where g_m' is the first derivative and g_m'' is the second derivative of the transconductance g_m with respect to the small signal input voltage v_i, respectively. Since the

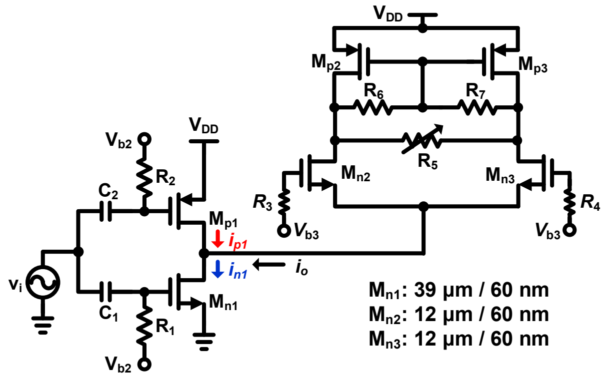

(a)

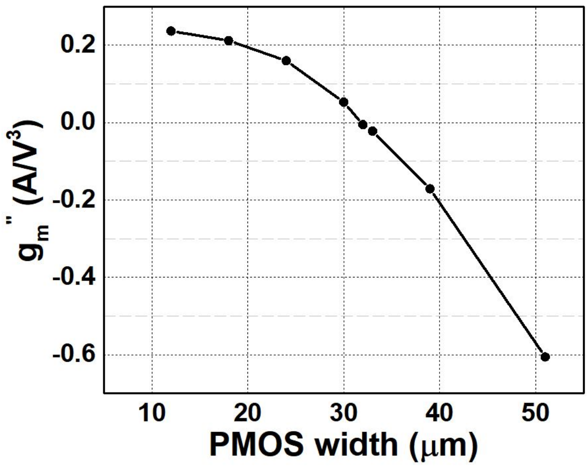

(b)

Fig. 6. (a) Inverter transconductor and switching transistors from down-conversion mixer, (b) g_m'' of small signal output current i_o of inverter transconductor versus the width of PMOS M_{p1} with a channel length of 65 nm.

third-order nonlinearity of CMOS circuit is dominated by g_m'' nonlinearity [10], $g_{m,n1}'' + g_{m,p1}''$ should be zero to achieve high linearity. By adjusting the proper size and bias point of PMOS M_{p1}, the $g_{m,n1}''$ term of NMOS M_{n1} can be cancelled by the $g_{m,p1}''$ term of PMOS M_{p1}. As shown in Fig. 6(b), when the width of PMOS M_{p1} with a channel length of 65 nm is approximately 32 μm, the second derivative g_m'' of the transconductance g_m with respect to the small signal input voltage v_i is zero.

Fig. 7 shows the simulated output-referred third-order intercept point (OIP3) of the proposed down-conversion mixer according to the width of PMOS M_{p1} with a channel length of 65 nm. The largest simulated OIP3 result of the down-conversion mixer is obtained when the width of PMOS M_{P1} with a channel length of 65 nm is approximately 35 μm. The proposed I/Q down-

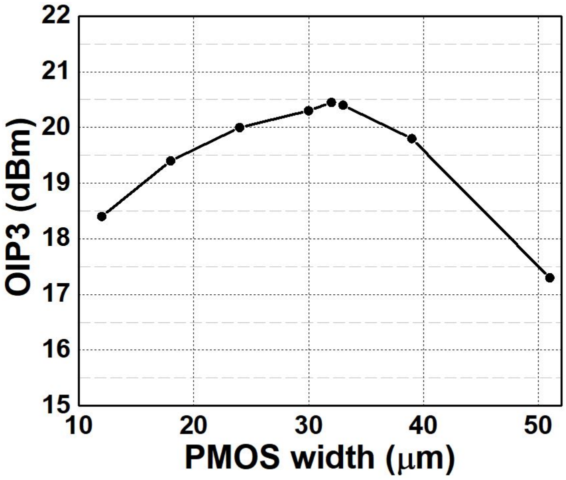

Fig. 7. Simulated OIP3 result of the proposed down-conversion mixer versus the width of PMOS M_{p1} with a channel length of 65 nm.

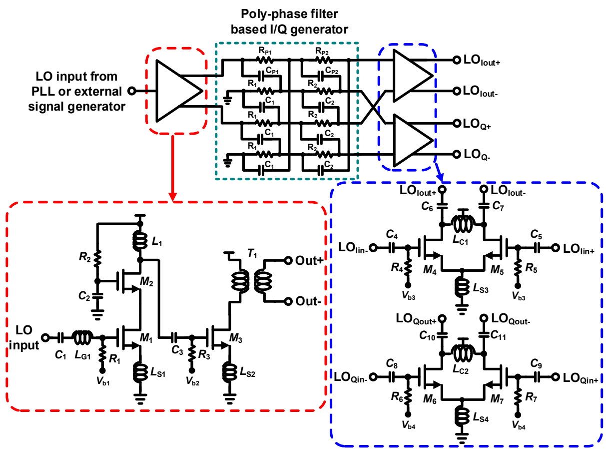

Fig. 8. Simplified schematic of the *I*/*Q* LO generation circuit.

conversion mixer improves more than 3 dB OIP3 performance in comparison to the conventional *I*/*Q* down-conversion mixer with an NMOS transconductor.

The balancing accuracy between the *I* and *Q* paths is critical in achieving the targeted signal-to-noise ratio in the direct-conversion receiver. Especially, it is important to obtain balanced *I*/*Q* LO signals in the millimeter-wave band [11]. Fig. 8 shows the simplified schematic of the *I*/*Q* LO generation circuits. The *I*/*Q* LO generation circuit consists of a single-ended cascode amplifier, a single-to-differential common-source amplifier, two-stage RC polyphase filter (PPF), and two differential common-source amplifiers. These amplifiers are used to compensate for the signal attenuation by two-stage PPF composed of passive components and to drive the switching pairs of the down-conversion mixer. The values of the resistance and capacitance of the two-stage PPF are destermined by considering the parasitic inductance value from equation in [12].

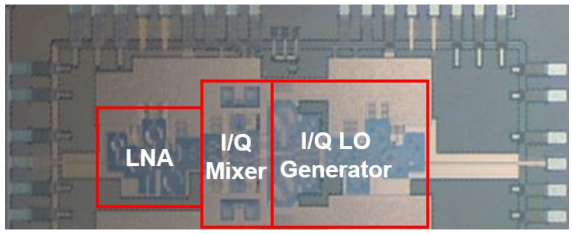

Fig. 9. Chip photograph of the receiver front-end.

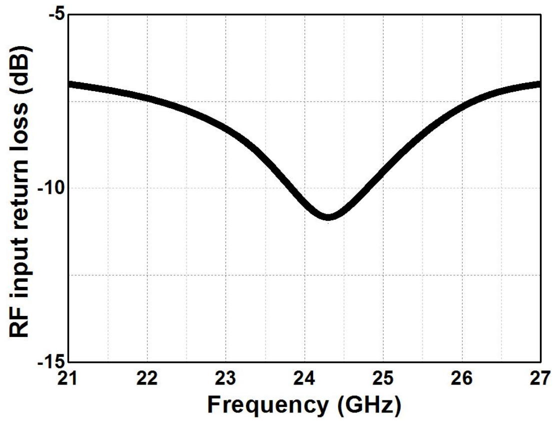

Fig. 10. Measured RF input return loss of the RF front-end.

III. Experimental Results

The proposed 24-GHz direct-conversion receiver front-end was implemented using a 65-nm CMOS process as part of an in-cabin radar system. Fig. 9 shows the chip photograph of the receiver front-end. The silicon area of the receiver front-end is 1250 μm × 550 μm excluding ESD protection circuits and PADs. It draws 21-mA from a 1.2-V supply voltage. For the measurement, an external signal generation instrument is used to provide the LO input signal. The measured return losses of the RF input and LO input are less than -10 dB in the frequency range from 24 GHz to 24.5 GHz.

Fig. 10 presents the measured RF input return loss of the RF front-end, which is less than -10 dB from 24 GHz to 24.5 GHz. Fig. 11 shows the measured conversion gain and phase mismatch between the *I*-path and *Q*-path at the IF output with an IF of 10 MHz of the RF front-end versus RF input frequency. The RF front-end shows a conversion gain of greater than 30 dB in the frequency range of 24 - 24.5 GHz. The gain and phase mismatch

Table 1. Summary and Comparison of Performance

	[8]	[9]	[10]	This work
Operating frequency (GHz)	24	25	24	24
Gain (dB)	31.5	15	36.7	30.4
OIP3 (dBm)	18.5	-4.4(1)	21.1	20.2
NF (dB)	6.7	9.5	6.1	4.5
P_{1dB} (dBm)	-24	-29	-29.7	-23
Power consumption (mW)	78 @ 1.2V (LNA + I/Q mixer + VCO & dividers)	20 @ 1.2V (LNA + I/Q mixer + LO generator)	66 @ 1.5V (LNA + I/Q mixer + LO generator)	25.2 @ 1.2V (LNA: 8 mA + I/Q mixer: 4 mA + LO generator: 9 mA)
Technology	65 nm CMOS	130 nm CMOS	130 nm CMOS	65 nm CMOS
Area	0.24 mm^2	0.84 mm^2	1.76 mm^2	0.69 mm^2
F.O.M(2)	0.15	0.05	0.19	1.35

(1) OIP3 ≈ Gain + IIP3 (= P_{1dB} + 9.6dB),

(2) $$F.O.M. = \frac{Gain[abs] \cdot IIP3[mW]}{P_{DC}[mW]} \cdot \frac{1}{(NF-1)[abs]} \cdot f[GHz]$$

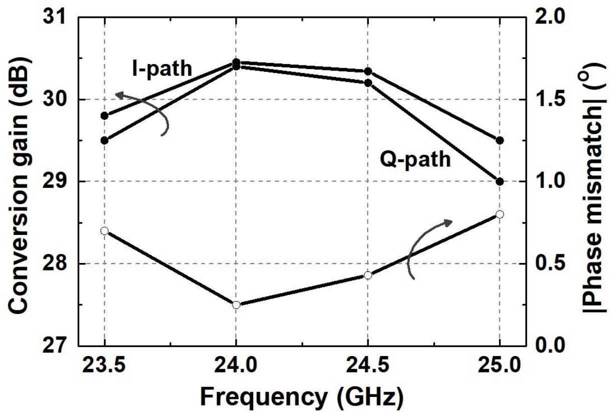

Fig. 11. Measured conversion gain and phase mismatch between *I*-path and *Q*-path at the IF output of the proposed RF front-end.

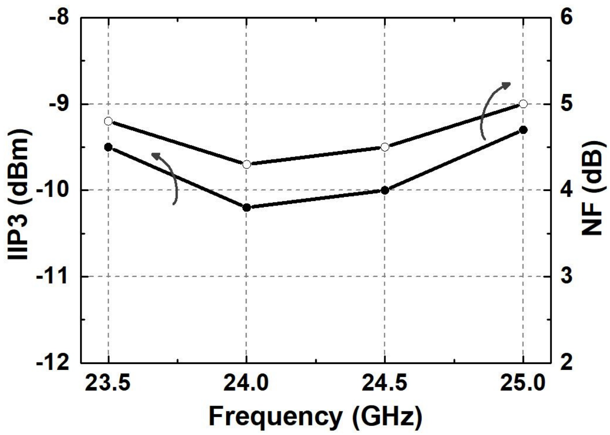

Fig. 12. Measured IIP3 and DSB NF of the proposed RF front-end versus operating frequencies.

between the *I*- and *Q*-paths at the IF output are less than 0.2 dB and 0.5° in the frequency range from 24 GHz to 24.5 GHz, respectively.

Fig. 12 shows the measured IIP3 and double-side band (DSB) noise figure (NF) results of the proposed RF front-end, respectively. Two-tone spacing is 2 MHz for the linearity test. The RF front-end has an IIP3 of greater than -10 dBm over the entire operating frequency bands. The RF front-end has a DSB NF of less than 4.5 dB over the entire operating frequency bands.

Table 1 summarized and compares the performances of the proposed RF front-end with those of other published mm-wave RF front-ends. The proposed RF front-end has good figure of merit (FOM) compared with the recently published millimeter-wave RF front-ends.

IV. CONCLUSIONS

A 24-GHz direct-conversion receiver front-end was presented for in-cabin applications. The proposed RF receiver is composed of a low-noise amplifier, an *I*/*Q* down-conversion mixer, and an *I*/*Q* LO generator circuit. An inverter transconductor with third-order nonlinearity cancellation is applied to the *I*/*Q* down-conversion mixer to improve the linearity of the *I*/*Q* down-conversion mixer. By adopting a linear *I*/*Q* down-conversion mixer and a balanced *I*/*Q* LO generator, the 24 GHz receiver front-end obtains high linearity and good *I*/*Q* balancing performance. The mm-wave receiver front-end can be utilized to in-cabin radar systems that can monitor driver's vital signs such as heart rate and respiration.

ACKNOWLEDGEMENT

This work was supported by the National Research Foundation of Korea (NRF) grant funded by the Ministry of Science and ICT (NRF-2019R1A2C1090935).

This research was supported by National R&D Program through the National Research Foundation of Korea (NRF) funded by Ministry of Science and ICT (2020M3H2A1078045).

This research was supported by Korea Institute for Advancement of Technology (KIAT) grant funded by the Korea Government (MOTIE) (P0012451, The Competency Development Program for Industry Specialist).

The CAD tools were supported by IDEC.

REFERENCES

[1] A. Droitcour, V. Lubecke, J. Lin, O. Boric-Lubecke, "A microwave radio for doppler radar sensing of vital signs," *In Proceedings of the 2001 IEEE MTT-S International Microwave Symposium Digest, Phoenix, AZ, US,* pp. 175-178, May 2001.

[2] Y. Xiao, J. Lin, O. Boric-Lubecke, M. Lubecke, "Frequency-tuning technique for remote detection of heartbeat and respiration using low-power double-sideband transmission in the ka-band," *IEEE Trans. Microw. Theory Tech.,* vol. 54, no. 5, pp. 2023-2032, May 2006.

[3] J.-H. Park, Y.-J. Jeong, G.-E. Lee, J.-T. Oh, J.-R. Yang, "915-MHz continuous-wave doppler radar sensor for detection of vital signs," *Electronics*, vol. 8, no. 5, pp. 855, May 2019.

[4] N. Andersen, K. Granhaug, "A 118-mW pulse-based radar SoC in 55-nm CMOS for non-contact human vital signs detection," *IEEE J. Solid State Circuits*, vol. 52, no. 12, pp. 3421-3433, Dec. 2017.

[5] T. N. Nguyen and H.-K. Cha, "Design of a low-power 10-bit 250-kS/s SAR ADC for neural recording applications," *IEIE Trans. Smart Process. Comput.*, vol. 10, no. 1, pp. 67-73, Feb. 2021.

[6] I. Nam, K. Choi, J. Lee, H.-K. Cha, B.-I. Seo, K. Kwon, and K. Lee, "A 2.4-GHz low-power low-IF receiver and direct-conversion transmitter in 0.18 µm CMOS for IEEE 802.15.4 WPAN applications," *IEEE Trans. Microw. Theory Tech.*, vol. 55, no. 4, pp. 682-689, Apr. 2007.

[7] A. Khan, "Electro-static Discharge(ESD) Tutorial," Cypress Semiconductor Corp, https://www.cypress.com/documentation/white-papers/electro-static-discharge-esd-tutorial.

[8] A. Karanicolas, "A 2.7 V 900 MHz CMOS LNA and mixer," *IEEE J. Solid State Circuits*, vol. 31, no. 12, pp. 1939-1944, Dec. 1996.

[9] C. Choi, K. Kwon, I. Nam, "A 370 µW CMOS MedRadio receiver front-end with inverter-based complementary switching mixer," *IEEE Microw. Wirel. Compon. Lett.* 2016, 26, 73-75.

[10] I. Nam, B. Kim, K. Lee, "CMOS RF amplifier and mixer circuits utilizing complementary characteristics of parallel combined NMOS and PMOS devices," *IEEE Trans. Microw. Theory Tech.*, vol. 53, no. 5, pp. 1662-1671, May 2005.

[11] B. Shin, C. Kim, O. Lee, S. Park, S. Noh, I. Nam, "A 24 GHz receiver front-end with improved I/Q balanced LO generator in 65-nm CMOS for surveillance radar systems," *Journal of Semiconductor Technology and Science*, vol. 18, no. 4, pp. 475-479, Apr. 2018.

[12] S. Lee, Y. Jeon, G. Park, J. Myung, S. Lee, O. Lee, H. Moon, I. Nam, "A 24-GHz RF transmitter in 65-nm CMOS for in-Cabin radar applications," *Electronics*, vol. 9, no. 12, pp. 2005, Dec. 2020.

Yangji Jeon received the B.S. degree in electronic engineering from Pukyong National University, Busan, Korea, in 2017, and the M.S. degree in electrical engineering at Pusan National University, Busan, Korea. Her main interests are CMOS RF/mmWave/analog circuits for wireless communications.

Suyeon Lee received the B.S. degree in electrical engineering from Pusan National University, Busan, Korea, in 2020 and is currently working toward the M.S. degree in electrical and electronics engineering at Pusan National University, Busan, Korea. Her main interests are CMOS RF/mmWave/analog circuits for wireless communications.

Jinman Myung received the B.S. degree in Electronic Engineering from Dong-A University, Busan, Korea, in 2019, and he is currently pursuing the combined M.S/Ph.D. degree in Electrical Engineering at Pusan National University, Busan, Korea. His main interests are CMOS RF/mmWave/PMIC/analog circuits for wireless communications.

Geonwoo Park received the B.S degree in Information and Communication Engineering from Kyungsung University, Busan, Korea, in 2019 and currently working toward the M.S. degree in Electrical Engineering at Pusan National University, Busan, Korea. His main interests are CMOS RF/mmWave/analog circuits for wireless communications.

Seungjik Lee received the B.S. degree in Electronic Engineering from Gyeongsang National University, Gyeongsangnam-do, Korea, in 2019, and the M.S degrees in Electrical Engineering from Pusan National University, Busan, Korea, in 2021, and is currently working toward the Ph.D. degree in Electrical and Electronic Engineering at Pusan National University, Busan, Korea. His current research interests are CMOS RF/PMIC/analog circuits for wireless communications.

Ockgoo Lee received the B.S. degree in electrical engineering from Sungkyunkwan University, Korea, in 2001, the M.S. degree in electrical engineering from the KAIST, Korea, in 2005, and the Ph.D. degree in electrical and computer engineering from the Georgia Institute of Technology, USA, in 2009. Upon completion of the doctoral degree, he joined Qualcomm Inc., USA, as a Senior Engineer, where he was involved in the development of transmitters and integrated passive circuits on mobile applications. He is currently a faculty member with the Department of Electrical Engineering, Pusan National University, Korea. His research interests include high-frequency integrated circuits and system design for wireless communications and biomedical applications.

Hyunwon Moon received a B.S. degree in radio science and engineering from Hanyang University, Korea, in 1997 and M.S. and Ph.D. degrees in EECS from KAIST, Korea, in 1999 and 2004, respectively. In 2004, he joined Samsung Electronics, Gyeonggi, Korea, as a senior engineer, designed multi-band multi-mode RF transceiver ICs for a cellular phone, and developed a receiver IC for a wireless connectivity system such as GPS and FM. In 2012, he joined the school of Electronic and Electric Engineering, Daegu University, Gyeongsan, Korea, as an associate professor. His research interests including CMOS RF/mmWave/analog integrated circuits and systems for wireless communications such as WSNs and 5G cellular systems.

Ilku Nam received the B.S. degree in electronics engineering from Yonsei University, Korea, in 1999, and the M.S. and Ph.D. degrees in electrical engineering and computer sciences from the KAIST, Korea, in 2001 and 2005, respectively. From 2005 to 2007, he was a Senior Engineer with Samsung Electronics, Gyeonggi, Korea, where he was involved in the development of mobile digital TV tuner IC. In 2007, he joined the School of Electrical Engineering, Pusan National University, Busan, Korea, and is now a Professor.